

Fixed-rate-breaking All-optical OFDM System using Time-domain Hybrid PAM with Sparse Subcarrier Multiplexing and Power-loading for Optical Short-reach Transmission

Takahiro Kodama^{1,2}, Akihiro Maruta², Naoya Wada³, and Gabriella Cincotti⁴

1. Faculty of Engineering and Design, Kagawa University, 2217-20 Hayashi-cho, Takamatsu, Kagawa 761-0396, Japan

2. Department of Electrical, Electronics and Information Engineering, Osaka University, 2-1 Yamada-oka, Suita, Osaka 565-0871, Japan

3. National Institute of Information and Communications Technology (NICT), 4-2-1 Nukui-Kitamachi, Koganei, Tokyo 184-8795 Japan

4. Engineering Department, University Roma Tre, via Vito Volterra 62, I-00146 Rome, Italy

tkodama@eng.kagawa-u.ac.jp

Abstract: All-optical TDHP-OFDM system with four-sparse-subcarrier-multiplexing and power-loading has been proposed for data-rate-adaptive transmission. 40-Gbit/s, 60-Gbit/s, and 80-Gbit/s can be selected by changing the ratio of PAM2 and PAM4, and all BERs achieve the FEC limit.

© 2020 Takahiro Kodama, Akihiro Maruta, Naoya Wada, and Gabriella Cincotti

1. Introduction

To reduce both capital expenditure (CAPEX) and operating expenditure (OPEX), network operators and system vendors are pushing more and more toward flexible data-rate transmissions, by changing the operating mode by software. The combination of optical and digital signal processing is a winning approach that can support emerging bandwidth-consuming applications, thanks to the drastic improvement of the performances of both optical and electrical analog components, such as SiO₂-based optical waveguides and digital signal processors (DSP).

Orthogonal frequency division multiplexing (OFDM) can adaptively handle the different Internet of the Things (IoT) signals, suitably assigning corresponding subcarriers [1,2]. However, the electrical discrete Fourier transform (DFT) and inverse DFT (IDFT) require high-power consumption, and an all-optical (AO) signal processing, using passive optical arrayed waveguide gratings (O-AWG) and 10Gbaud-based opt-electrical analog components, can reduce both power consumption and system costs [3,4]. Previous experiments of an eight subcarrier AO-OFDM system, with two-ary pulse amplitude modulation (PAM2) and differential phase-shift keying (DPSK), have been demonstrated by using two paired O-AWGs; however, this approach requires optical-domain chromatic dispersion (CD) monitoring and compensation [5]. CD-compensation-free AO-OFDM transmission is limited to less than 20 km, because, after propagation, the intensity peaks of the subcarriers shift from the null points of the other sub-channels, so that relative time delay among the subcarriers breaks the channel orthogonality [6]. Time- and frequency-domain sparse subcarrier multiplexing with a narrow-spaced optical frequency comb and subcarrier selection have been proposed by reducing the linear crosstalk due to CD among adjacent subcarriers [7]. However, the approach is bandwidth inefficient and not flexible, since it is difficult to change the subcarrier pattern adaptively; besides, each subcarrier is assigned to a single modulation format. A straight solution is to use time-domain hybrid modulation, that suitably adapt the data rate and transmission reach while keeping the baud rate and subcarrier pattern constant [8].

We propose a transparent time-domain hybrid PAM (TDHP) using 10 Gbaud 2^m-ary PAM. TDHP can flexibly configure OFDM signals, according to the difference between the required signal to noise ratio (SNR) at the forward error correction (FEC) limit, and the dispersion tolerance; besides, the variety of DSP operating modes and opt-electrical analog components can be minimized. We reduce the implementation complexity, and enhance the system scalability, with simple management. TDHP with the single carrier has been demonstrated to present high tolerance to noise and dispersion, compared to PAM4 signal for point-to-point transmission; however, the performance of AO-OFDM and the TDHP optimization have not been reported.

In this paper, we propose a power loading TDHP signal, consisting of the conventional PAM2 and PAM4 signals. We experimentally demonstrate a bit error rate (BER) performance improvement by power loading in a TDHP-based 60 Gb/s OFDM system, using a narrow-spaced optical frequency-comb and paired O-AWGs, over 40 km single-mode fiber (SMF) dispersion-compensation-free transmission.

2. Time- and frequency-domain sparse subcarrier multiplexing

The O-AWG impulse response and corresponding transfer function are

$$h_k(t) = \sum_{n=0}^{N-1} e^{-2\pi j \frac{nk}{N}} \delta\left(t - \frac{n}{C}\right) \quad H_k(f) = \sum_{n=0}^{N-1} e^{2\pi j \frac{n}{C}\left(f - k\frac{C}{N}\right)} \quad k = 0, 1, \dots, N-1$$

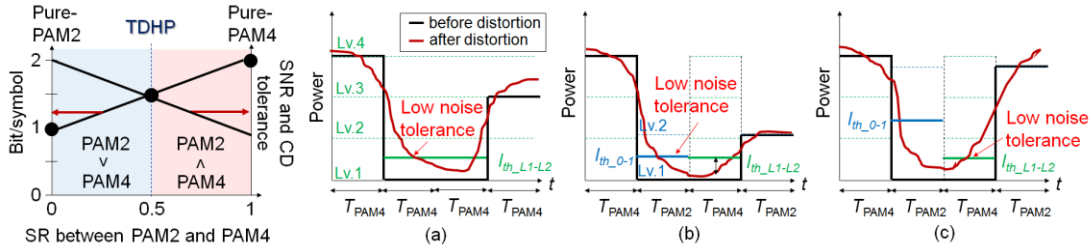


Fig. 1. Data rate and tolerances relation Fig. 2. Noise tolerances (a) standard PAM4, (b) PAM4 dominant TDHP, (c) PAM2 dominant TDHP.

where $\mathbf{j}=\sqrt{-1}$, $\delta(t)$ the Dirac delta function, N the port number, k the output port, and C is the free spectral range (FSR). In the standard OFDM, the frequency comb spacing Δf_{comb} coincides with the O-AWG *sinc* spacing C/N [Hz], and the waveform has a time duration of N/C [s], that can be distorted by inter-symbol interference (ISI). Perfect orthogonality is achieved only at the center of a symbol time, where the SC intensity peak coincides with the null points of the other SCs, that occurs only in the back-to-back (B-t-B) case.

In the proposed time and frequency sparse subcarrier OFDM, the cavity length of frequency comb laser source is flexibly controlled, and the comb spacing decreases from Δf_{comb} to $\Delta f'_{\text{comb}}$. To increase the SC spacing, the signal output is turned off by the optical LN-IM modulator during the time assigned to the unused subcarrier. Since $\Delta f'_{\text{comb}} < C/N$, the SC spacing is the lowest common multiple of $\Delta f'_{\text{comb}}$ and C/N . In time waveform increases of a factor $\Delta f_{\text{comb}}/\Delta f'_{\text{comb}}$, so that ISI is mitigated and crosstalk effect from adjacent subcarriers is drastically reduced. Therefore, the proposed AO-OFDM is suitable for CD compensation-free long-reach transmission.

3. Power-loading

Figure 1 shows the tradeoff between data rate and SNR and CD tolerance, as a function of the symbol ratio (SR) between PAM2 and PAM4. PAM4 presents low tolerance to noise and CD, and the transmission reach is limited to a short distance. As shown in Fig. 2(a), the waveform spreading of the highest intensity level causes symbol error. For a single carrier transmission, with the optimized modulation format between PAM2 and PAM4, the performance of TDHP signal can be equalized, and the transmission reach extended. Here, the SR is set to 0.5, corresponding to the intermediate data rate between pure PAM2 and PAM4. The optimization of the optical power of the TDHP signals at the transmitter allows us to achieve the best performance. If the PAM2 signal power is lower than the optimum, as shown in Fig. 2(b), the noise tolerance of PAM2 is degraded by the ISI of PAM4 due to the CD. On the other hand, if the PAM2 power is higher than the optimum, as shown in Fig. 2(c), the noise tolerance of PAM4 is degraded by ISI of PAM2 due to CD.

4. Experiment

Figure 3 shows the experimental setup and results of four-subcarrier $\times 10$ GSymbol/s TDHP-OFDM transmission without dispersion compensation through an SMF with 0.18 dB/km attenuation and 17 ps/nm/km dispersion parameter. A narrow-band (NB) optical bandpass filter with 1.6 nm 3 dB bandwidth was placed at the O-AWG output, to tailor the signal spectrum. Two O-AWGs with a 200 GHz free spectral range were placed at the transmitter and the receiver. The erbium-doped fiber amplifiers (EDFA) were used to compensate for the insertion losses. The sampling rates in the electrical arbitrary waveform generator (E-AWG: Tektronix, 7122C) and digital sampled oscilloscope (DSO: Keysight, DSAX96204Q) were 10 GSa/s and 80 GSa/s, respectively. A mode-locked laser diode (MLLD) was used as a comb light source, with a 10 GHz repetition rate at 1550 nm central wavelength, and generated a 2.4ps optical pulse stream, as shown in Fig. 3(a). Each power-spacing and peak-to-peak adjusted PAM2 and PAM4 signals with 100000 symbol test data was generated by E-AWG and modulated into a data sequence by the Lithium Niobate-intensity modulator (LN-IM). At the AO-OFDM transmitter, four-subcarrier OFDM signals were generated at the O-AWG outputs #1, #5, #9 and #13, and were combined by the couplers. The polarization and powers of all the subcarriers were equalized by polarization controllers (PCs) and variable optical attenuators (VOAs). The four subcarrier OFDM signals correspond to subcarriers number #1, #2, #3, and #4, respectively, and Fig. 3(b) reports the multiplexed signal before the SMF transmission.

At the receiver side, the signal was launched into the O-AWG to separate the subcarriers; the subcarrier #2 spectrum is shown in Fig. 3(c). The received signals were detected by a photodetector (PD) having 7.5 GHz 3 dB bandwidth and sampled and quantized by the DSO. The offline processing emulates the receiver-side DSP, and the sampled and quantized signal was equalized by a least mean square (LMS) algorithm that compensates for degradation effects due to bandwidth limitation of opt-electrical analog components, such as digital to analog converter (DAC), analog to digital converter (ADC), PD and RF driver amplifier. We observe that only in the case of the optimal peak power ratio (PR) between PAM2 and PAM4, the PAM4 signal was not degraded by the data pattern effect and bandwidth

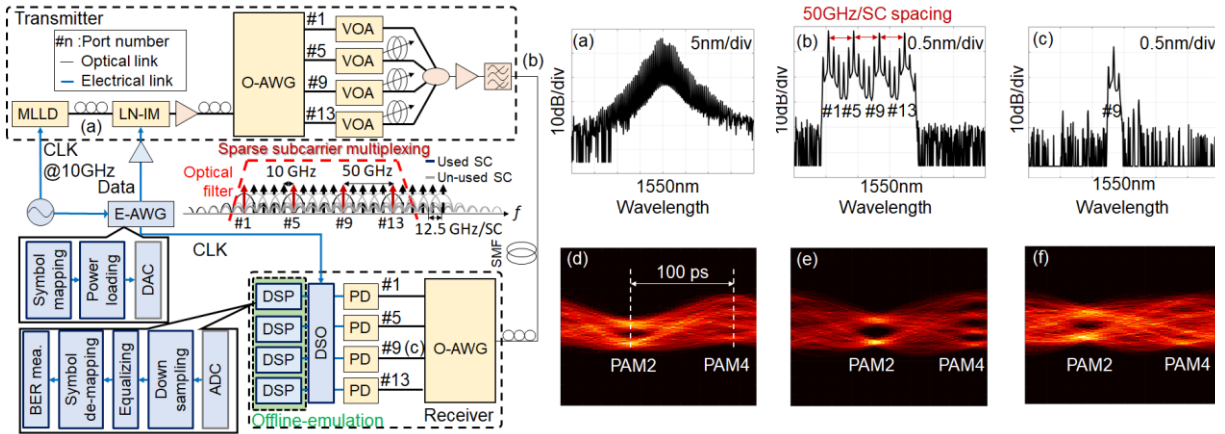


Fig. 3. Experimental setup and results a) optical frequency comb spectra, (b) sparse subcarriers OFDM spectrum, (c) received subcarrier #3 spectrum, (d) TDHP waveform (B-to-B, PR = 0.2), (e) TDHP waveform (B-to-B, PR = 0.6), (f) TDHP waveform (B-to-B, PR = 1).

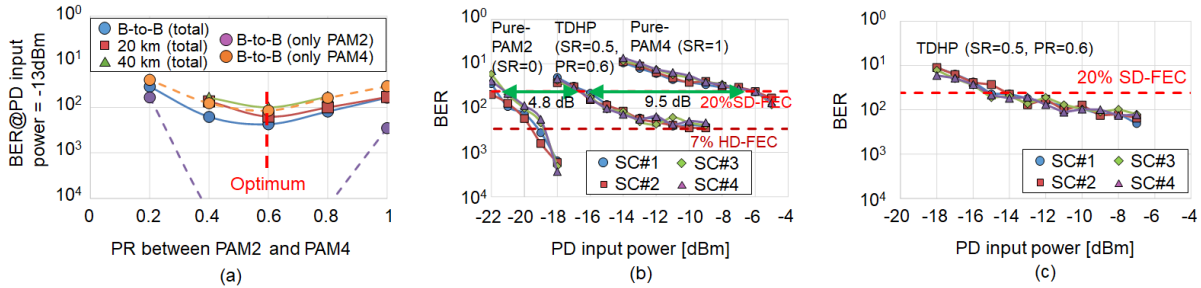


Fig. 4. Measured BERs (a) TDHP signal performance as a function of peak PR, (b) B-to-B case, (c) 40 km SMF transmission case.

limitation of the optical and electrical analog components (see Figs 3(d-f)). The system performances were finally evaluated by BER calculation after a hard decision while adjusting received signal power at PD input.

Figure 4(a) shows the measured TDHP BERs for three transmission distances in the case of -13 dBm received power as a function of peak PR. The optimum peak PR between PAM2 and PAM4 was found to be 0.6, and it was independent of the transmission distance. Increasing or decreasing the PAM2 PR from the optimum peak PR, both of PAM2 and PAM4 BER values became decreasing.

Figure 4(b) shows the measured BERs of pure-PAM2, TDHP, and pure-PAM4, four subcarriers multiplexed signal, for B-to-B case. As before, the optimal peak PR of TDHP was 0.6. The three different BER characteristics were due to different SNR tolerance of the modulation formats. We associate two different FECs (20% soft-decision FEC (SD-FEC) threshold (2.4×10^{-2}) and 7% hard-decision FEC (HD-FEC) threshold (3.4×10^{-3}) to achieve error-free operation. We define the power penalty as the receiver sensitivity difference at $\text{BER} = 2.4 \times 10^{-2}$. The power penalty between pure-PAM2 and TDHP was 9.5 dB. The power penalty between TDHP and pure-PAM4 was 4.8 dB. The only pure-PAM2 signal was achieved the FEC limit of 7% HD-FEC.

Figure 4(c) shows the measured BERs of the TDHP, four subcarriers multiplexed signal, for 40km SMF transmission without CD compensation. We measured 2.5 dB power penalty due to the 40 km SMF transmission. As the signal power increases, the high level of the TDHP signal was corrupted by shot noise. Therefore, the optimum spaced eye pattern setting was useful to improve the system performance at high power.

5. Conclusions

We have achieved a fixed-rate-breaking AO-OFDM system for the first time. This configuration allows us to flexibly change the data rate from 40 Gb/s to 80 Gb/s with a fixed baud rate and a number of subcarriers. Four sparse subcarriers, 60 Gb/s, TDHP-OFDM transmission using a narrow-spaced optical frequency-comb and paired O-AWG at a single wavelength over dispersion-free 40 km SMF transmission has been successfully demonstrated.

References

- 1 W. Shieh *et al.*, *Opt. Express* **16**(2), 841-859, (2008).
- 2 K. Christodouloupoulos *et al.*, *JLT* **29**(9), 1354-1366, (2011).
- 3 K. Takiguchi *et al.*, *Opt. Lett.* **36**(7), 1140-1142, (2011).
- 4 I. Kang *et al.*, *Opt. Express* **19**(10), 9111-9117, (2011).
- 5 A. Lowery *et al.*, *Opt. Express* **20**(9), 9742-9754, (2012).
- 6 K. Yonenaga *et al.*, *in Proc. OFC*, paper JthA48, (2008).
- 7 T. Kodama *et al.*, *in Proc. OFC*, paper W3I.3, (2019).
- 8 S. Ohlendorf *et al.*, *in Proc. ECOC*, paper Mo3F.6 (2018).